Astron. & Astrophys. 48, 421—435 (1976)

High Resolution Studies of Spiral and Irregular Galaxies at 2695 and 8085 MHz II: NGC 1569 and NGC 891

E. R. Seaquist and R. C. Bignell
David Dunlap Observatory and National Radio Astronomy Observatory

Received July 4, revised December 17, 1975

Summary. We present aperture synthesis observations of the irregular galaxy NGC 1569 and the edge-on spiral NGC 891 at 2695 and 8085 MHz. The approximate resolution at these two frequencies are 9″ nad 3″ respectively. In both cases the radio emission is similar to the optical form of the galaxy, and contains a mixture of thermal and nonthermal components. Furthermore, the brightest source in each galaxy is nonthermal, and is probably synchrotron radiation.

The radiation detected from NGC 1569 is predominantly thermal emission from large H II regions some of which are also evident in Hα.

The luminosity of the nucleus and the disk emissivity for NGC 891 are larger than that of typical spiral galaxies, but are consistent with van der Kruit's (1973) relation between these two quantities.

Key words: galaxies — radio emission

1. Introduction

We present here aperture synthesis observations of the irregular galaxy NGC 1569 and the edge-on spiral NGC 891 at 2695 and 8085 MHz. The observations were carried out with the three-element interferometer of the National Radio Astronomy Observatory[1]) at Green Bank, West Virginia. The technique used in the observations and data reduction, and the UV plane coverage are identical to that described in paper I (Seaquist *et al.*, 1975). The maps presented possess the highest resolution yet available for these galaxies and the data are therefore suitable for investigating the distribution of both brightness temperature and the spectral index.

2. The Radio Maps

The radio maps for the two galaxies at 2695 and 8085 MHz are shown in Figs. 1, 2, 7 and 8. In addition, the radio contours for NGC 1569 are superimposed on Hα and continuum photographs of this galaxy in Figs. 3 and 4. The photographs were supplied by P. W. Hodge (private communication). The 2695 MHz contours for NGC 891 are superimposed in Fig. 9 on a photograph of this galaxy supplied by S. van den Bergh (private communication). The overlay procedure and accuracy achieved in positioning are discussed in paper I.

The radio maps do not show features whose angular extents exceed 4′ and 1′.3 at 2695 and 8085 MHz respectively, since they are resolved by the largest fringe spacings used (100 m baseline). An exception in NGC 891 occurs since the source is highly elongated and the galactic ridge is parallel to interferometer fringes over some portion of the UV track.

Each map has been deconvolved by the process known as "cleaning" (see paper I) in order to reduce the level of confusion by sidelobes and grating rings. The first grating ring is at the 10% level with radius 1′.3 (0′.4) at 2695 (8085) MHz, so that the maps are inevitably aliassed, particularly at 8085 MHz. "Cleaning" constitutes a model fitting procedure and does not provide a unique model of the UV plane data. The "clean" iterations were stopped when either 200 components were removed or when the amplitude of the cleaned components reached 5% of the maximum amplitude on the map. All maps shown contain both the clean components and the residuals which remain after cleaning. The clean beam parameters used are shown in Table 1.

Table 1. Clean beam parameters for NGC 1569 and NGC 891

	Frequency (MHz)	Beam dimensions (arcs)	Position angle of major axis (degrees)
NGC 1569	2695	7.7 × 5.5	−42
	8085	3.0 × 2.1	−34
NGC 891	2695	9.8 × 4.5	−39
	8085	3.7 × 1.8	−38

[1]) The N.R.A.O. is operated by Associated Universities Inc. under contract to the National Science Foundation.

To assess the reliability of the cleaning procedure, we subjected the clean maps (including those used to obtain spectral information, discussed later) to two tests. First, the clean components were transformed to the UV plane and subtracted from the interferometer data. The residuals were then transformed to produce a new intensity map, which would contain only noise if the clean components exactly represented the true brightness distribution. The resulting mean residual brightness for NGC 1569 and 891 were respectively about 5% and 15% of the peak brightness on the original clean maps. We conclude that some of the clean maps are probably confused by grating rings at and below these levels, but that the clean components above these levels form a good fit to the UV plane data.

Second, the transformed clean components for each map were used to construct a simulated source of known brightness distribution which is similar to the true brightness distribution of the galaxy. Random noise was added in the UV plane to simulate the effect of receiver noise. The resulting UV map was transformed, cleaned, and then compared to the original clean map. In each case the mean difference in brightness between the original and final clean map is less than 10% of the peak brightness. This figure provides a second measure of the level of confidence to be applied when interpreting all of the radio maps considered in this paper. In particular, it forms an estimate of the degree of reliability with which the complex brightness distributions considered here can be cleaned in the presence of both noise and grating lobe confusion with the UV distribution actually used.

3. NGC 1569

(a) Previous Observations

NGC 1569 has been classified as a magellanic irregular (Holmberg, 1958; de Vaucouleurs, 1963) and appears to be associated with the Ursa Major-Camelopardalis Cloud (Ables, 1971). This association is based upon a distance of 3.3 Mpc derived by Ables from a study of the brightest stars and H II regions.

This galaxy has recently aroused interest because of the excellent photographs by Hodge (1974) which reveal a diverging pattern of Hα filaments in this object. Both Hodge and Zwicky (1971) have suggested that the origin of this phenomenon might be an explosive event within the galaxy. More recently, de Vaucouleurs *et al.* (1974) have discussed in some detail the evidence for an explosion in NGC 1569. In brief, they find support for this view from the existence of two bright centrally located blue star-like objects, a flat radio spectrum (abnormal for late-type irregulars), the existence of a compact radio source possibly coincident with one of the star-like objects, and finally, in the abnormal strength and chaotic velocity field of the Hα filaments. They suggest that one or the other of the blue stellar-like objects in the galaxy may be the point of ejection of the filaments, but this point is very uncertain. For example, Ables (1971) has suggested that they might be foreground stars.

Lequeux (1971) has shown from interferometric observations with east west resolution at 1420 MHz that the radio emission is resolved into an extended disk with $S = 0.30 \pm .05$ Jy and HPW = 2′.2, and an unresolved source (< 1′) with $S = 0.12 \pm .05$ Jy at 1950 coordinates $\alpha = 04^h26^m05^s.6$ (±0′.5), $\delta = +64°44'.4$ (±0′.1). The position of the unresolved source is nearly coincident with one of the star-like objects, although the accuracy of the position is insufficient for a certain identification.

(b) General Features

The 2695 MHz map in Fig. 1 shows a remarkable similarity to the isophotal maps in *B* and *V* produced by Ables (1971). For example, the major axis of the distribution of emission is 1′.3 in both bands if the −10 db contour in each case is used. The position angle of the major axis and the axial ratio derived from the outer radio contours are respectively 119° and 0.50. The corresponding figures given by Ables for the distribution of blue light are 116° and 0.49. The brightest part of the radio map is coincident with the brightest region in blue light shown in the contour maps presented by Ables. In Fig. 3a this region is occupied by diffuse emission coincident with the radio peak. This strong radio source, henceforth termed the nuclear source, is presumably the unresolved source described by Lequeux (1971). It does not coincide with either of the stellar candidates suggested by de Vaucouleurs *et al.*, nor do these candidates appear to coincide with any other feature of the radio emission. This observation strengthens the suggestion by Ables that they are foreground stars, although membership in the galaxy cannot yet be ruled out. The distribution of emission at 2695 MHz follows the general distribution of light in Hα as seen in Fig. 3b. As with blue light, the brightest region in Hα is coincident with the region of most intense radio emission (the nuclear source).

Figure 2 shows that the 2695 emission is resolved into smaller, mainly unresolved sources at 8085 MHz. The absence of any extended background at the higher frequency may be attributed in part to the effects of resolution by the interferometer (mentioned earlier). The individual components in the high resolution map also show some correspondence with features on the Hα photograph (Fig. 4b). The nuclear source which appears well resolved on this map coincides, as in the case at 2695 MHz, with the blue feature on Hodge's continuum photograph (Fig. 4a). Table 2 contains a list of the prominent sources and their characteristics.

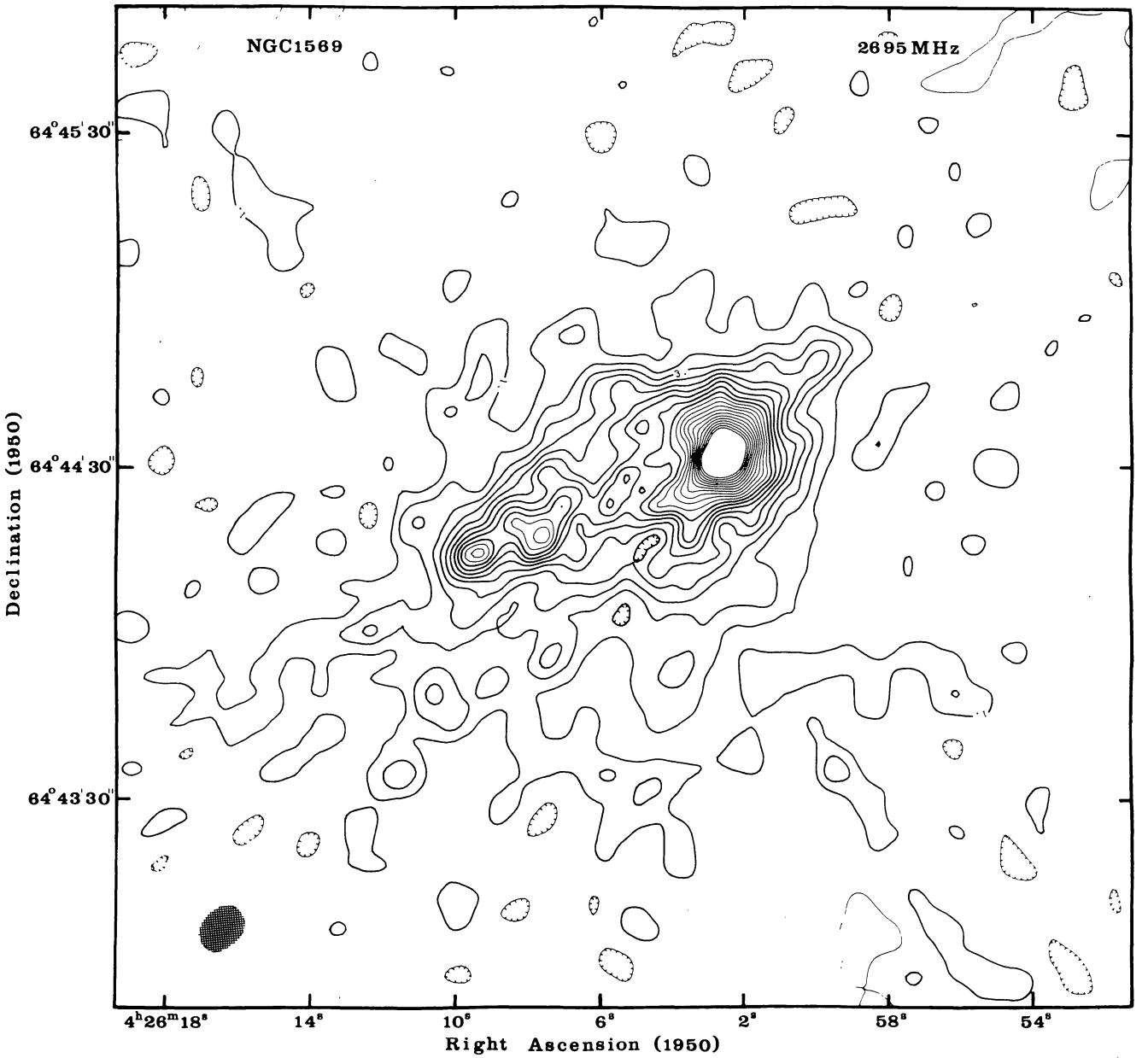

Fig. 1. 2695 MHz map of emission from NGC 1569. The zero contour and contours above twenty have been omitted. The peak brightness is thirty contours and the contour interval corresponds to an increment in brightness temperature of 1.9 °K

Table 2. A list of the stronger sources found in the 8085 MHz map of NGC 1569 in Fig. 2. The sources are classified as thermal and non-thermal. The classification is based on the spectral index profiles in Fig. 6 and/or association with Hα emission in Fig. 4

Source designation	Position (1950) R.A.	Dec.	S_{8085} (mJy)	Spectrum
A	$04^h26^m02^s.6$	64°44′01″	14.8	Nonthermal (with possible thermal mixed)
B	04 26 03.0	64 44 38	4.4	Thermal
C	04 26 03.5	64 44 27	6.3	Thermal
D	04 26 04.4	64 44 29	4.8	Thermal (?)
E	04 26 05.4	64 44 31	4.5	Thermal (?)
F	04 26 07.4	64 44 19	4.2	Thermal
G	04 26 08.4	64 44 21	4.3	Thermal

The general prominence of the features at the higher frequency, coupled with the general association of the 2695 MHz emission with the Hα brightness suggests that a substantial fraction of the observed radio emission in Fig. 2 is thermal in origin. We shall therefore examine the spectral index distribution of the emission using both our own maps and other available data on the integrated flux density.

(c) Spectral Index of the Observed Emission

The spectral index (defined by $S \propto \nu^{-\beta}$) is about 0.1 for thermal emission, and generally much larger (0.7) for nonthermal, or synchrotron radiation. Figure 5 shows the spectrum of NGC 1569 between 750 and 6630 MHz. Some of these data were obtained from Haynes *et al.*

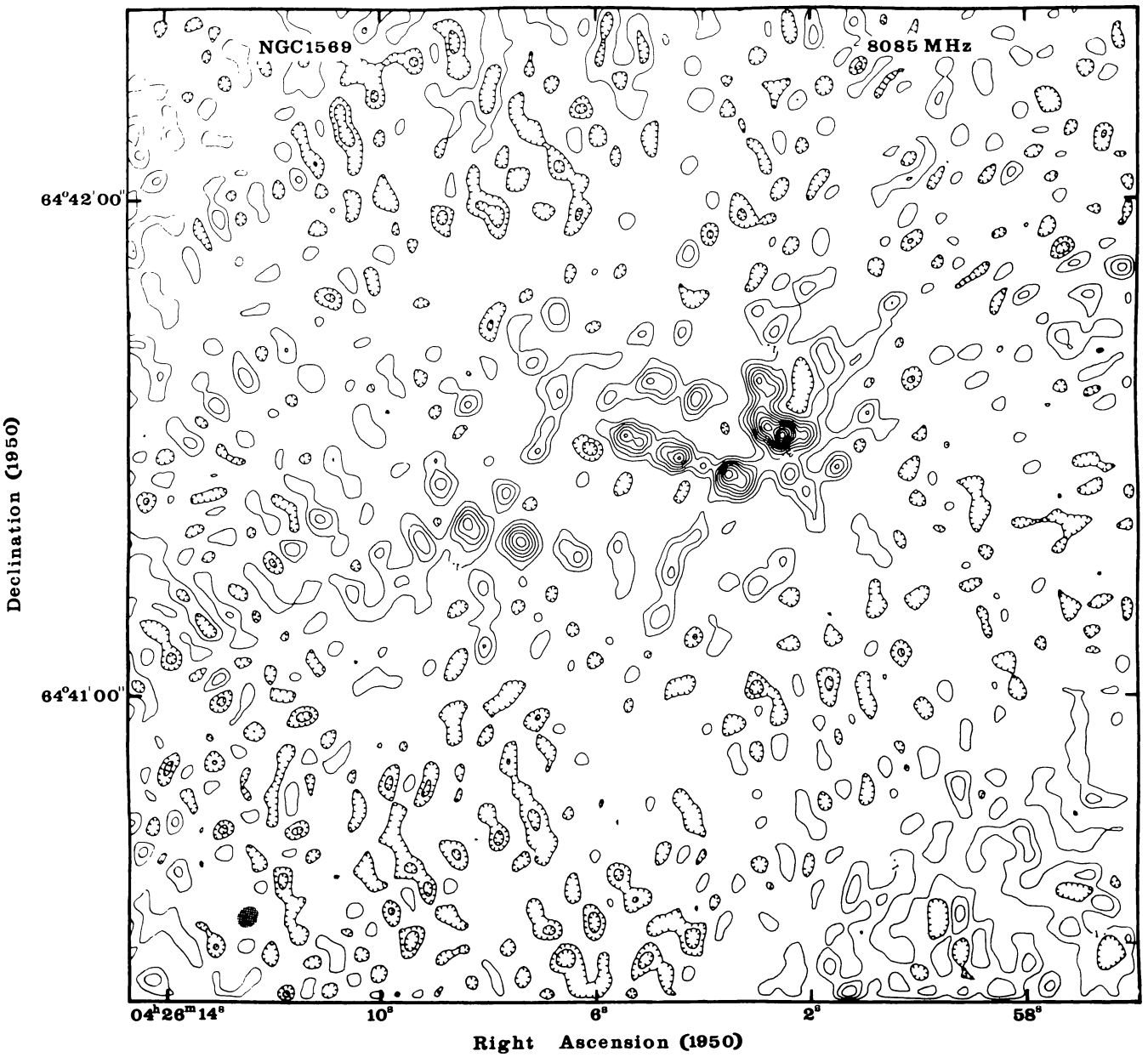

Fig. 2. 8085 MHz map of emission from NGC 1569. The zero contour has been omitted. The contour interval corresponds to an increment in brightness temperature of 1.1 °K

(1975). To their data we have added our own flux density (252 mJy ±15%) at 2695 MHz obtained by integrating the brightness contours of the map in Fig. 1. We have used also a 750 MHz flux density of 0.4 Jy from Heeschen and Wade (1964). These authors do not quote an error in their measurement and we assume a standard error of ±0.1 Jy to allow for the effects of confusion with their instrument. Figure 5 shows that the spectral index is not well determined, since the scatter at the higher frequencies is rather large. It is worth noting that our own point at 2695 MHz is an interferometric observation, and it appears low as would be expected if there is an extended component partially resolved by the interferometer. Kazes *et al.* (1970) give an east-west diameter of 3′.1 at 2695 MHz, which is comparable to our largest fringe spacing of 4′ at this frequency, and our own flux density is therefore likely to be an underestimate of the integrated flux. The measurement of McCutcheon (1973) at 6630 MHz is a peak flux density and has not been corrected for the source size which may be comparable to his beamsize. If this correction is made, and the interferometer point is removed, there is good evidence for a very flat spectrum, consistent with thermal emission from an optically thin ionized gas. It is also possible that the emission is synchrotron radiation from electrons with an unusually flat energy spectrum, but this possibility is less likely, in our view.

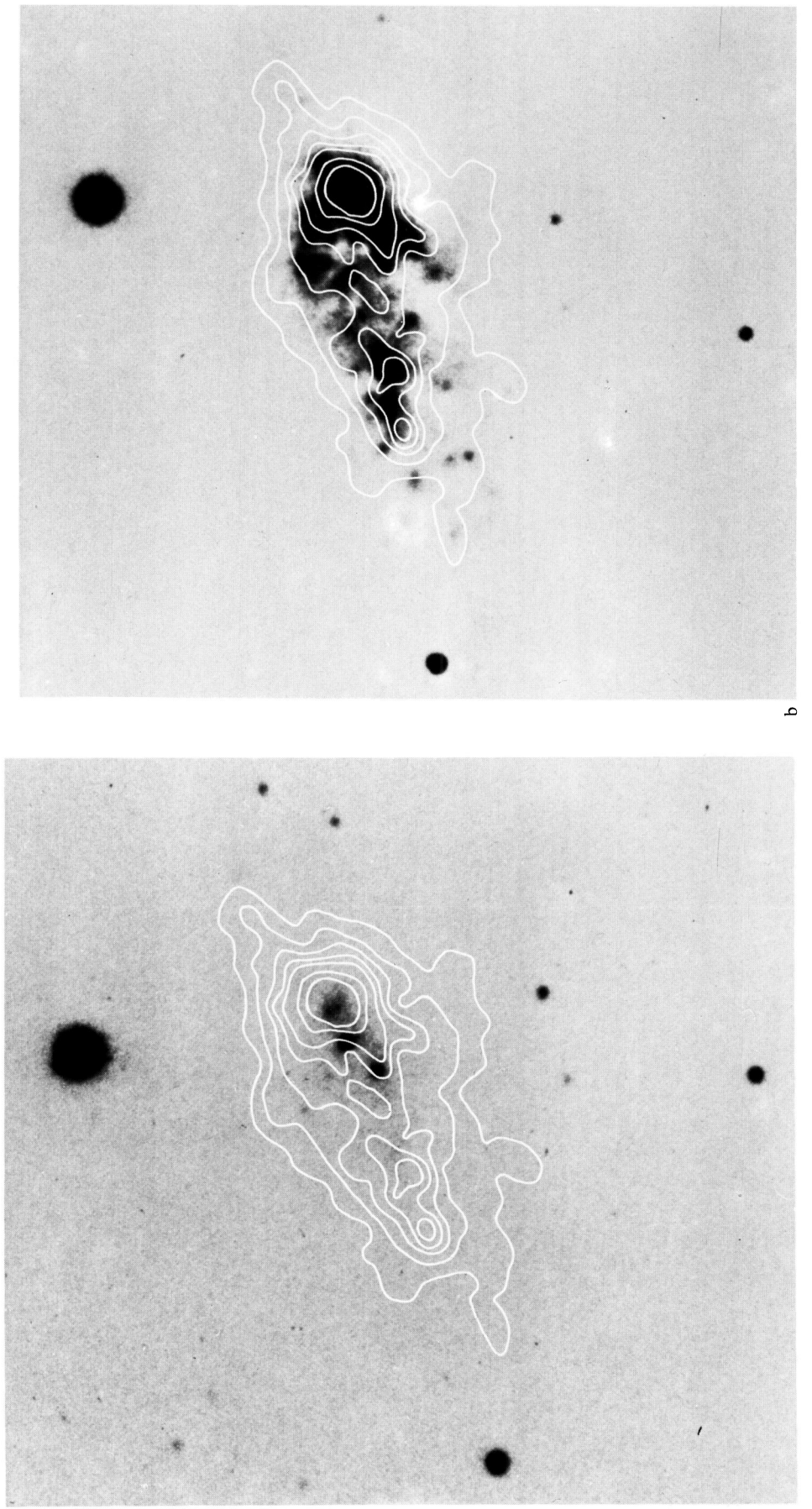

b

Fig. 3a and b. The 2695 MHz map of NGC 1569 superimposed on (a) the short exposure continuum photograph published by Hodge (1974); (b) the short exposure Hα photograph published by Hodge (1974). Some contours have been omitted for the purpose of clarity

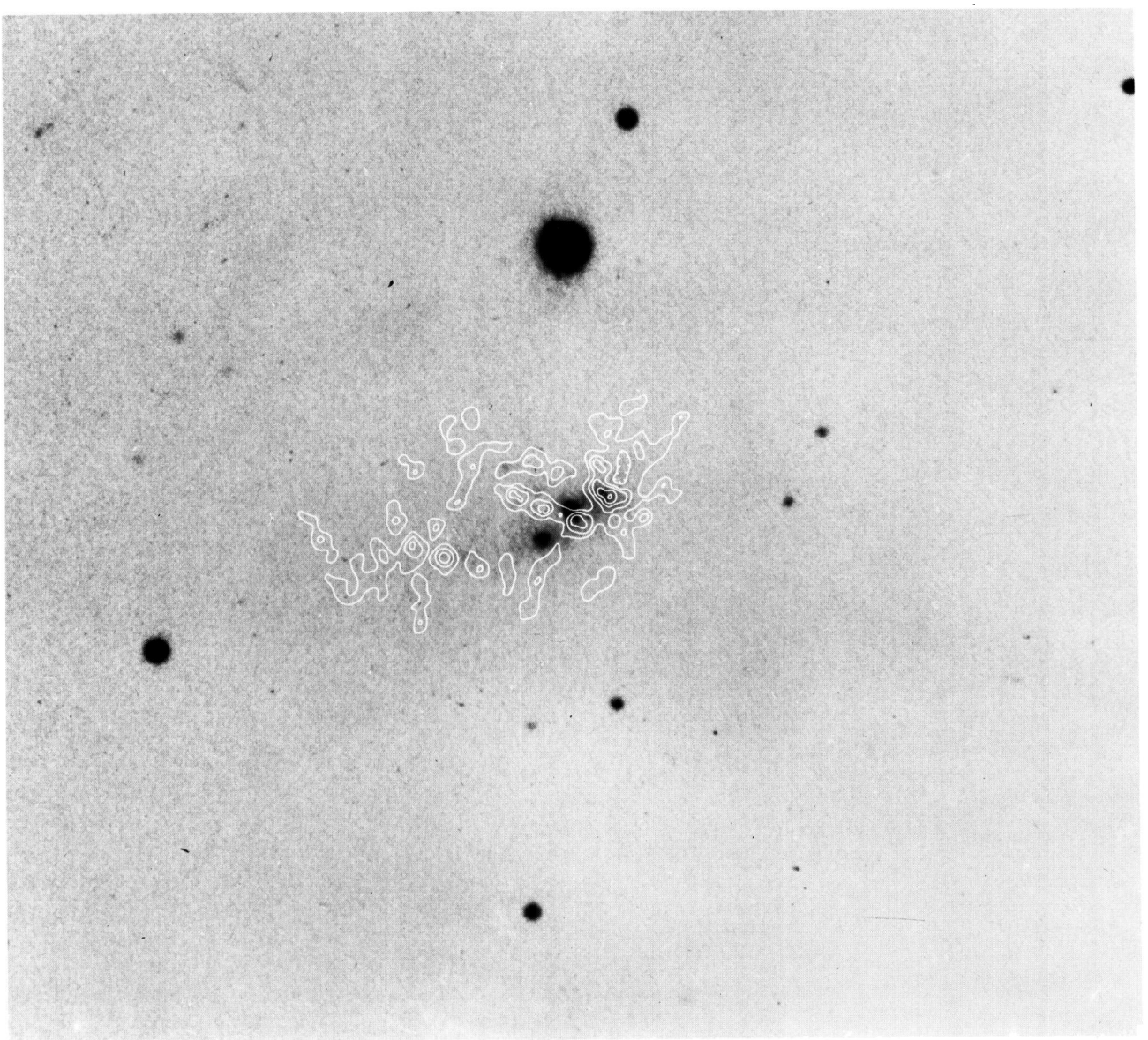

a

Fig. 4a and b. The 8085 MHz of NGC 1569 superimposed on the photographs in Fig. 3. Some contours have been omitted for the purpose of clarity

We may investigate the spectral index distribution in the galaxy between 2695 MHz and 8085 MHz using the interferometer maps. It is essential for this purpose to restrict the two maps to identical UV coverage. In Fig. 6 we present the resulting maps at each frequency in the form of brightness profiles in right ascension at intervals of 2.″8 in declination. Some caution is required in the interpretation of these profiles. They are somewhat noisier than the maps in the Figs. 1 and 2 (because of the restricted UV coverage). We have applied the tests discussed in Section 2 to these maps and the results given there are applicable here. We believe the brightness distribution of the stronger sources is real, and we shall consider only the more intense regions for examining the spectral index. The error bars shown are based on the rms noise on the maps.

There are several points worth noting in the profiles. First, the profiles dominated by the nuclear source in Fig. 1 ((b)–(h) inclusive) clearly show that this source contains a mixture of components with different spectral indices. In the brightest region, for example, the emission is nonthermal. Profiles (b), (c) and (f)–(h) show however that the spectrum of the emission immediately to the north and to the south east becomes flat, characteristic of thermal emission. This observation suggests that sources B and C (see Table 2) in the high resolution map of Fig. 2 are of thermal origin whereas the complex nuclear source A, or part of it, is nonthermal in origin. The spectral index defined by the intensity ratio at the peak brightness is 0.25. However, since the beam size is about 7″, this spectral index refers to the brightness smoothed over several thermal and

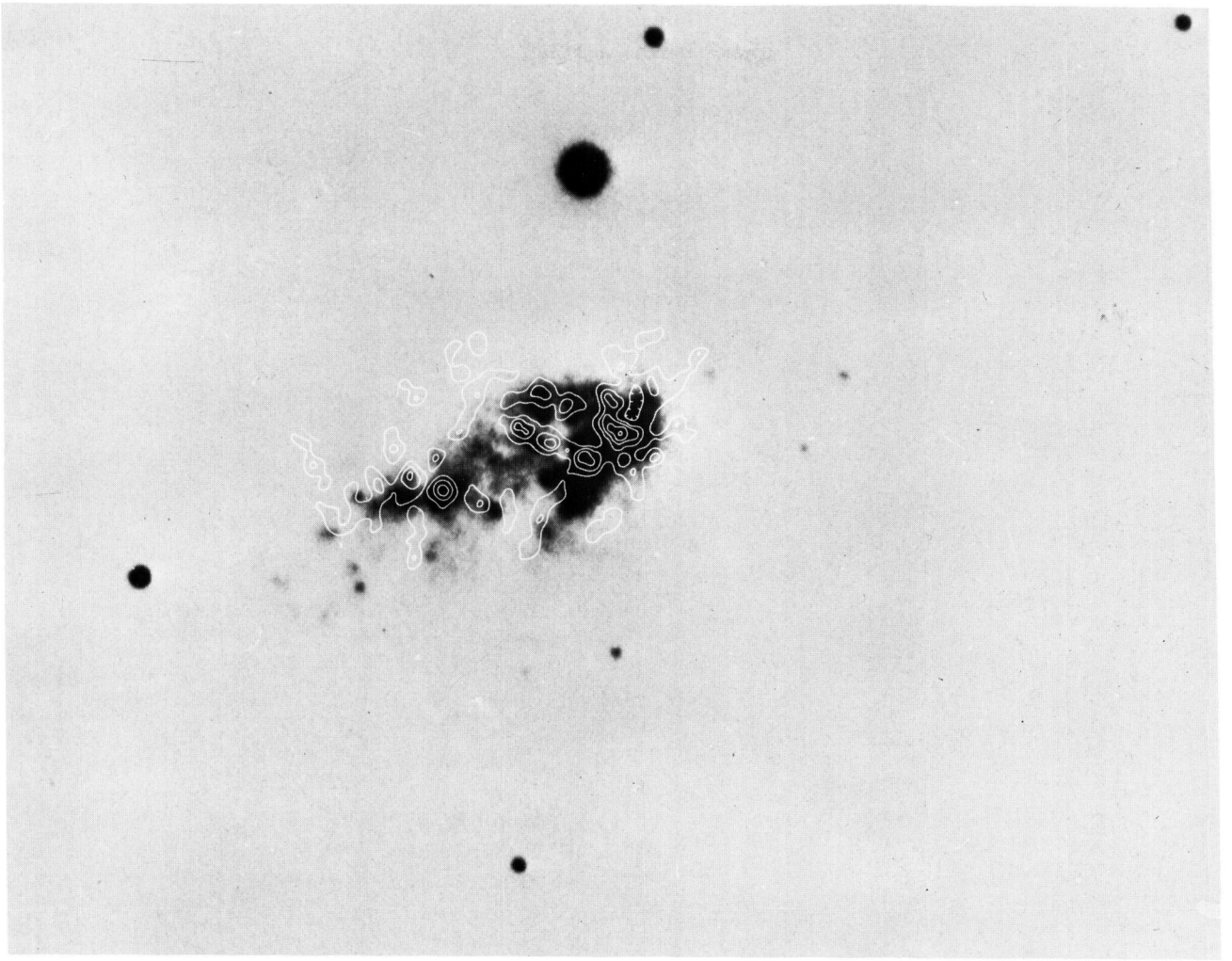

b

Fig. 4b

nonthermal components together and is therefore a lower limit to the spectral index of the nonthermal component. As a conservative estimate to the strength of the nonthermal component, we adopt for the flux density of the brightest component of source A in Table 1 a figure of 5 mJy at 8085 MHz.

Secondly, profiles (f)–(i) inclusive show a strong deficiency in 8085 MHz emission relative to that at 2695 MHz in an extended region centred on 1950 coordinates $\alpha = 04^h26^m06^s.0$, $\delta = +64°44'26''$. This may therefore be a region of predominantly synchrotron radiation. Similar, but less convincing regions exist south west of source A in the vicinity of 1950 coordinates $\alpha = 04^h26^m03^s.0$, $\delta = +64°44'22''$ (profiles (g)–(i)), and north east of this source at $\alpha = 04^h26^m03^s.8$, $\delta = 64°44'40''$. Thirdly, the two emission regions at the south eastern edge of the galaxy in Fig. 1 appear to have a thermal spectrum, as seen from profiles (h)–(l), though there is some evidence for nonthermal emission in the region between and below the two sources. The eastern component appears in Fig. 2 to be resolved into two components of equal strength (sources F and G in Table 2). The remaining areas are too weak to enable any firm conclusions concerning their spectrum.

The integrated flux densities derived from the spectral index profiles yield 123 ± 20 mJy and 107 ± 25 mJy at 2695 and 8085 MHz respectively. Note that the 2695 MHz flux density here is about one half that quoted earlier (252 mJy) for the flux obtained from Fig. 1. We attribute the difference to the restricted UV coverage used in the spectral index profiles. The flux densities quoted above yield a spectral index of 0.13 ± 0.25 which is consistent with the radio spectrum in Fig. 5 if the revisions suggested earlier are made to that figure.

The conclusion from the spectral index studies is that thermal emission plays an important and possibly a dominant role in the radio emission from this galaxy.

(d) Nature of the Individual Sources

As we have earlier pointed out, the nuclear source is resolved in Fig. 2 into a mixture of thermal and nonthermal components (sources A, B and C). The flux

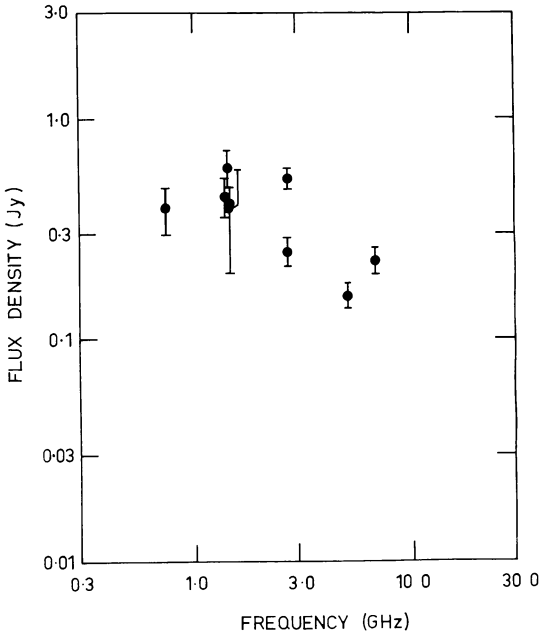

Fig. 5. The spectrum of the integrated flux density of NGC 1569 between 750 and 6630 MHz

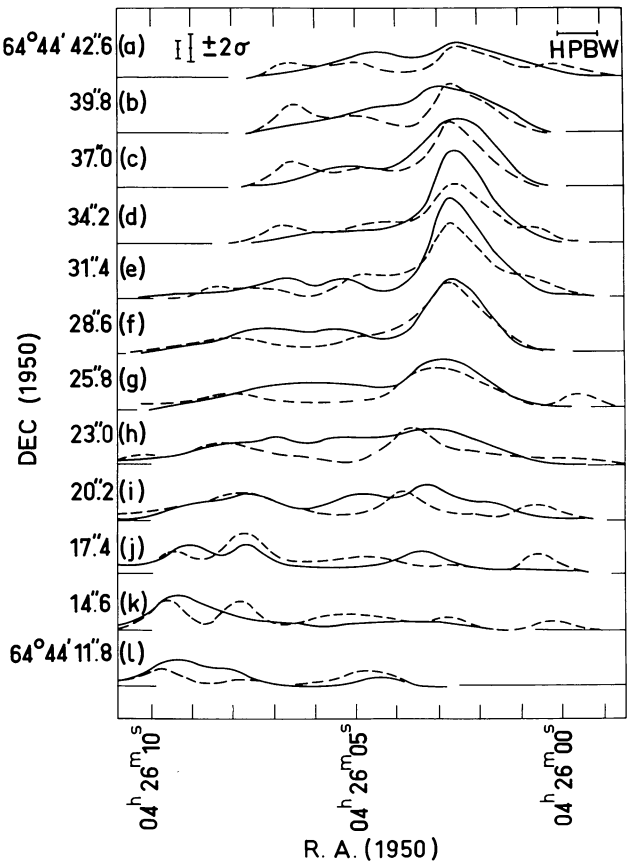

Fig. 6. Brightness profiles in right ascension for NGC 1569. Each profile shows both the 2695 MHz emission (———) and 8085 MHz emission (— — —). These profiles were constructed from maps with identical UV coverage and they possess a resolution comparable to that in Fig. 1. The error bars are based on the noise observed on the maps, and the larger error bar refers to the 8085 MHz (dashed) profiles

density at 2695 MHz measured above the 6th contour in Fig. 1 is 34 mJy, or about 13% of the integrated emission in this map. The high resolution map shows that the overall angular extent is 12″ which at 3.3 Mpc corresponds to a linear extent of 200 pc. If the brightest component of source A is assumed to be the nonthermal source then its flux density at 8085 MHz is 5 mJy, as mentioned earlier. If $\beta=0.7$ this source would possess a luminosity between 10^{7} and 10^{11} Hz of 3.6×10^{36} erg s^{-1}. For comparison the luminosity of the nonthermal source at the centre of our own galaxy (Sag A East) is 2.3×10^{35} erg s^{-1}, about an order of magnitude less.

It is interesting to note that there are some similarities between the nuclear source and the strong emission region MC 74 near the 30 Doradus region of the Large Magellanic Cloud (LMC). The latter source has an integrated spectral index of 0.2 (McGee and Newton, 1972) which suggests that it too is a mixture of thermal and nonthermal sources. MC 74, if placed at the distance of NGC 1569, would possess a flux density of 10 mJy at 2700 MHz and a half power angular extent of 7″, not unlike the nuclear source in NGC 1569. Furthermore, both sources are displaced with respect to the radio emission centroid of their respective galaxies.

The nature of the blue continuum feature associated with the nuclear source is unknown. The optical emission in Hodge's photograph (Fig. 3a) appears to be double, although this effect may be produced by variable extinction in this region. The emission could be produced by very blue stars, or by nonthermal emission associated with the radio source. In connection with the former possibility, it has been suggested by others (e.g. Smith *et al.*, 1972) that explosive events may trigger bursts of star formation in galaxies.

It is probable that most or all of the remaining strong sources in the 8085 MHz map are thermal, and are associated with large H II regions. Figure 4 shows that sources A, B, C, E, F and G overlie optical emission regions in Hα. Source D however appears almost coincident with a blob of interstellar dust which exhibits arms extending radially outward. The easternmost source on the 2695 MHz map does not appear to be associated with any H II region, although it is possible that the optical emission is obscured by dust. Adopting a distance of 3.3 Mpc for NGC 1569, we find that an H II region with a flux density of 4 mJy (typical of those in Table 2) possess a volume emission measure ($=\int N_e^2 dV$) of 1.6×10^{64} cm^{-3}. The largest H II regions in our own galaxy, such as Sgr B 2 and W 49, possess a volume emission measure of about 3×10^{63} cm^{-3}, so that the sources in NGC 1569 are indeed giant H II regions.

If we assume that all of the emission from NGC 1569 is thermal, then the required volume emission measure is 10^{66} cm^{-3}. Assuming the gas is distributed uniformly in a disk of diameter 2 kpc and height 0.4 kpc, we obtain a r.m.s. electron density of 5 cm^{-3}, and a mass of $1.7\times10^{8}\,M_{\odot}$. By comparison, the mass of neutral hydrogen for NGC 1569 given by Roberts (1969) is $3.7\times10^{8}\,M_{\odot}$ (corrected to 3.3 Mpc from 2.5 Mpc assumed by Roberts). It appears then that a very large fraction of the gas in this system is ionized. This result is consistent with the observation by de Vaucouleurs, de Vaucouleurs, and Pence (1974) that the intensity of the Hα emission in NGC 1569 is almost an order of magnitude greater than in the average magellanic irregular.

4. NGC 891

(a) Previous Observations

NGC 891 is an edge-on Sb spiral galaxy belonging to the NGC 1023 group. The distance to this group is about 14.3 Mpc (Sandage and Tammann, 1975). Holmberg (1958) gives $m_{pg}=10.85$ corrected for galactic and internal absorption, and this photographic magnitude combined with the above distance yields $M_{pg}=-19.9$. The disk of this galaxy shows the presence of a dust layer whose filaments extend up to heights of 1 kpc (the Z-direction) above the plane of the galaxy (Sandage, 1961), which possibly indicates that the magnetic field extends to this height also.

Baldwin and Pooley (1973) have carried out observations of NGC 891 with the Cambridge One-Mile Telescope at 408 MHz with a synthesized HPBW of 80″ in r.a. by 120″ in dec. Although the resolution is rather poor, these authors succeeded in showing that the extent of emission in the Z-direction is 5 kpc (corrected to 14.3 Mpc from their assumed 7 Mpc), comparable to or greater than the extent of the dust filaments. They also show that the radial distribution of emissivity at 408 MHz is more highly peaked toward the centre of NGC 891 than in our own galaxy, which indicates the presence of a relatively stronger radio emitting region near the nucleus.

(b) General Features

The map in Fig. 7 bears a strong resemblance to radio maps of the plane region of our own galaxy. The distributions of optical and infrared brightness also bear a resemblance to photographs of the plane of our own galactic system as has been pointed out by Osterbrock and Sharpless (1952). The point of maximum radio brightness, which is possibly at the nucleus of the galaxy, is located at 1950 coordinates $\alpha=02^{h}19^{m}24\overset{s}{.}9\pm0\overset{s}{.}2$, $\delta=42°07'18''\pm2''$. This is near the optical position for the nucleus of NGC 891 given by Gallöuet *et al.* (1973) which is $\alpha=02^{h}19^{m}24\overset{s}{.}6$, $\delta=+42°07'12''$. There is an unresolved source at the above radio position which is surrounded by a region of enhanced emission. Both sources are in turn superimposed upon the galactic ridge emission which is coextensive with the optical disk (see Fig. 9).

The higher resolution 8085 MHz map in Fig. 8 has a low signal to noise ratio, and shows only sources in the brighter regions near the nucleus. Although it is not possible therefore to learn much about the structure of the individual sources in the disk, other than the nuclear source, this map does show prominent emission regions which agree in position with the brighter emission regions in Fig. 7.

An examination of Fig. 9 shows very few instances, if any, of a detailed correspondence between radio and optical features. The lack of correlation is not surprising since the dominant feature of the galactic ridge is the dust lane which obscures optical emission from the H II regions in both the spiral arms and the nucleus of the galaxy.

(c) The Spectrum of the Radio Emission

Figure 10 shows the radio spectrum of the radiation integrated over the entire galaxy. The data of this figure are from Haynes *et al.* (1975). To their data we have added our own flux density at 2695 MHz of 0.48 ± 0.03 Jy, obtained by integrating the contours in Fig. 7. We have not added a corresponding point at 8085 MHz since much of the emission is resolved out at this frequency. From Fig. 10 we observe that our 2695 MHz flux density is in good agreement with that predicted by the radio spectrum derived from all the points representing the integrated emission from NGC 891. It is unlikely therefore that more than about 15% of the emission remains undetected in our interferometer map at 2695 MHz. The spectrum plotted in this figure yields a spectral index of 0.79 which shows that the radiation from this galaxy is predominantly nonthermal over most of the frequency range displayed.

We may examine the spectrum of individual features by comparing maps at the two frequencies. As pointed out earlier, however, the signal-to-noise ratio at 8085 MHz is low and therefore an extensive comparison is not possible. Nevertheless, it is possible to make some conclusions, particularly about the nuclear region. Figure 11 shows a comparison of brightness profiles at the two frequencies. These two profiles were prepared from maps restricted to identical UV coverage, and each profile represents a brightness distribution which is strip integrated in right ascension across the plane of the galaxy. The latter procedure was used to improve the signal-to-noise ratio at the expense of resolution in right ascension. Although the differences in brightness between the two curves are of the order of the error in one sampling point, there are areas where the 8085 MHz profile is systematically lower, which indicates that the

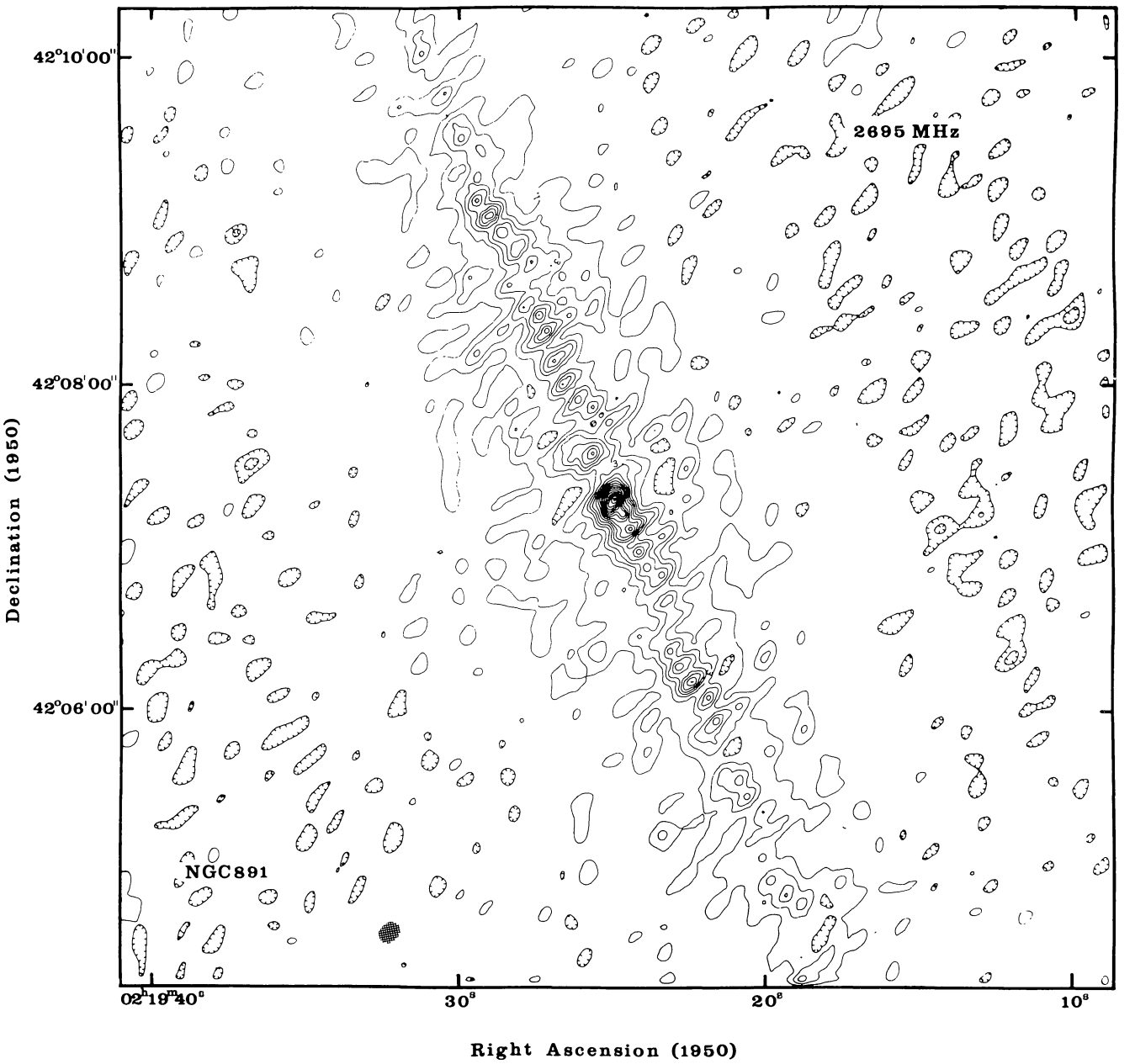

Fig. 7. Map of 2695 MHz emission of NGC 891. The zero contour has been omitted, and the contour interval is equivalent to an increment in the brightness temperature of 2.2 °K

difference in brightness in these areas is significant. The shapes of the two profiles remain similar however and this characteristic adds weight to the reality of the observed difference. The unresolved nuclear source in particular is nonthermal. The brightness ratio at the 2695 MHz peak is 1.93 which corresponds to a spectral index of 0.60. This is not the spectral index of the nuclear source alone however since the disk component has not been subtracted. There is evidence that a significant fraction of the radiation extending to a distance of 20″ (1400 pc) on either side of the nucleus is nonthermal as well.

The radiation further than 20″ from the nucleus shows a possible mixture of thermal and nonthermal sources, but the individual sources are too weak to permit their spectral index to be determined. There is some suggestion that the 2695 MHz emission is composed of a base disk component with individual sources superimposed upon it, while the 8085 MHz emission is composed of sources with a much weaker base disk emission. The presence of noise on the higher frequency profile adds significantly to this impression, however. This behaviour is consistent with a structure in which thermal radiation, emitted by large H II regions in the

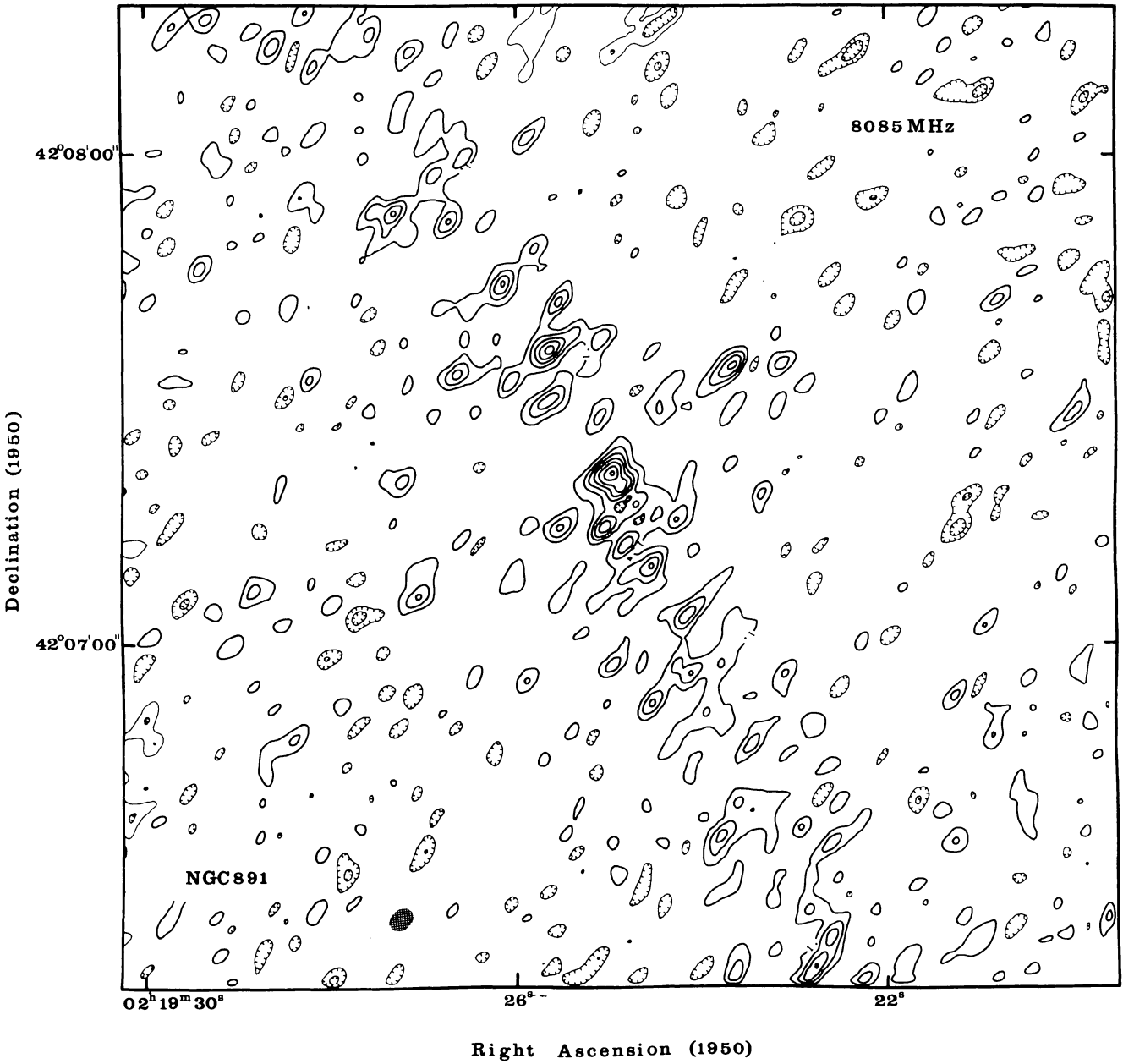

Fig. 8. Map of 8085 MHz emission of NGC 891. The zero contour has been omitted, and the contour interval is equivalent to an increment in the brightness temperature of 1.3 °K

spiral arms is superimposed upon a smoother nonthermal base disk.

The integrated flux densities contained in the profiles in Fig. 7 are 125 ± 7 mJy and 81 ± 10 mJy respectively at 2695 and 8085 MHz, yielding a spectral index is 0.39 ± 0.17. Since this is much less than the spectral index derived from Fig. 10 the proportion of the radiation in Fig. 11 which is thermal must be correspondingly larger. For example, if the spectral index of the nonthermal component alone is assumed to be 0.79, the observed value of 0.39 requires that about 50% of the 2695 MHz radiation be thermal in Fig. 11. However, since the total flux density is 480 mJy at 2695 MHz there is a component undetected in Fig. 11, and this fraction for the percentage thermal emission may not be representative of the entire galaxy. In fact, unless the percent thermal emission in this undetected component is significantly less than 50%, the spectrum in Fig. 10 would exhibit considerable flattening at frequencies above 1400 MHz. In the absence of any significant flattening, we conclude that 50% is an upper limit to the fraction of the total 2695 MHz radiation which is thermal. A lower limit to this fraction is obtained by assuming on the other hand that all of the radiation in the undetected component is nonthermal. This assumption gives about 13%, so that 13–50% of

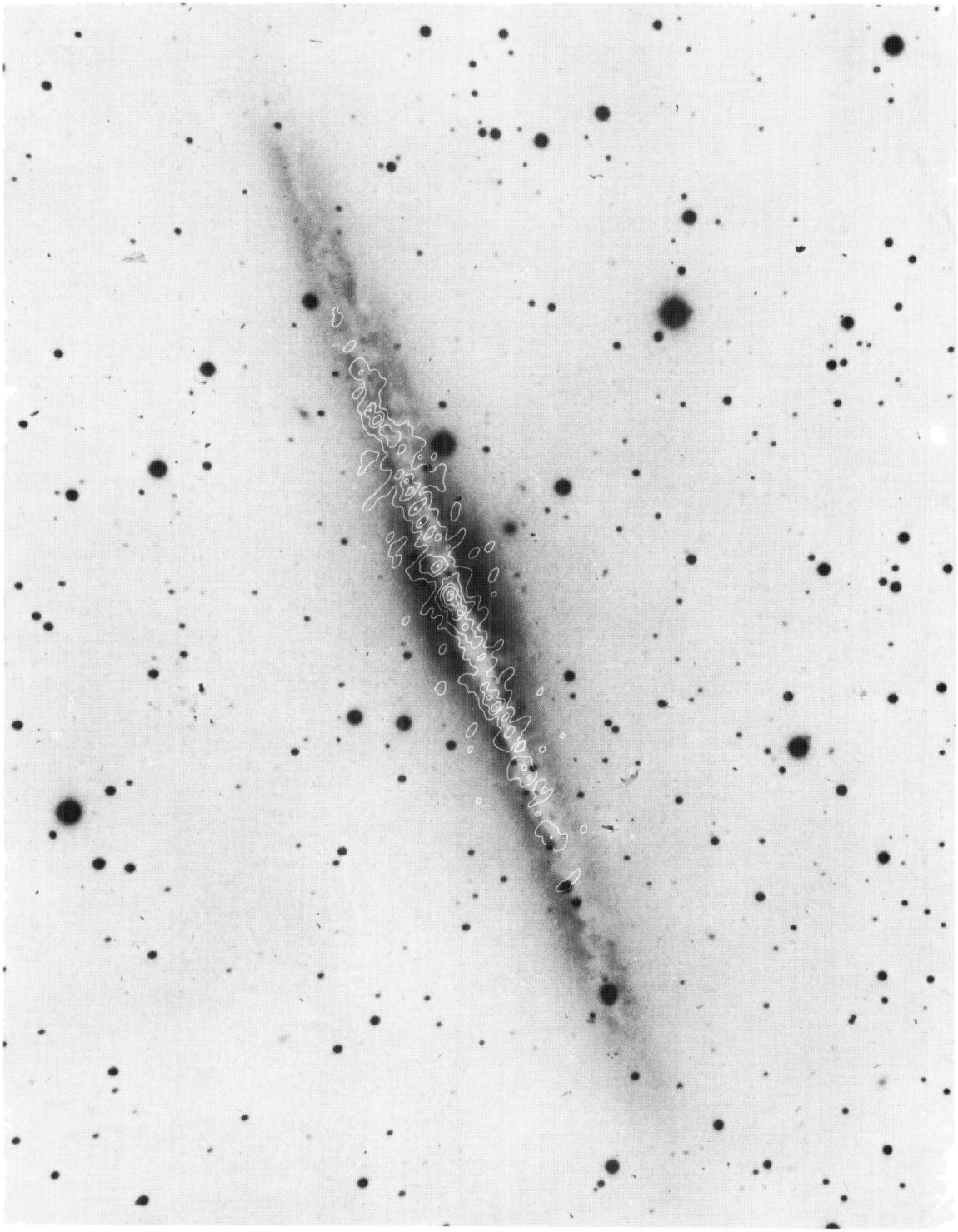

Fig. 9. The 2695 MHz map superimposed upon a photograph of NGC 891 taken with the 200-inch telescope of the Hale Observatories by S. van den Bergh. Some contours have been omitted for the sake of clarity

the total radiation at 2695 MHz is thermal in origin. This figure is similar, though perhaps somewhat lower than similar estimates for M 31 (Berkhuijsen and Wielebinski, 1974) and our own Galaxy (Hirabayashi *et al.*, 1972).

(d) The Nuclear Region

The nuclear region (within a few hundred parsec of the nucleus) is composed of an unresolved source with a half power width less than 5″ (350 pc) and a flux density

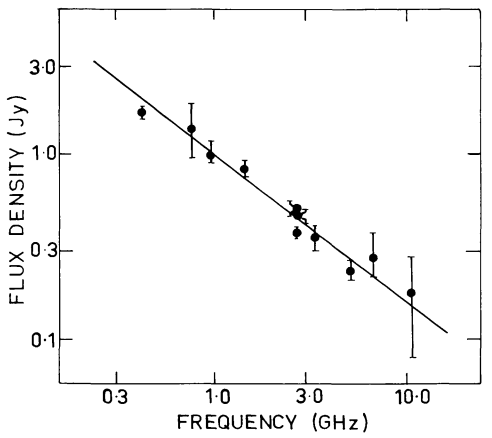

Fig. 10. Spectrum of the integrated flux density of NGC 891. The line drawn through the points corresponds to a spectral index of 0.79

of 4 mJy superimposed upon an extended region with a half power width of about 20″ (1400 pc). These two components, both of which are nonthermal, are in turn superimposed upon the underlying galactic disk radiation.

The structure of the nucleus at higher resolution is shown at 8085 MHz in Fig. 8. The peak brightness in this map is located at 1950 coordinates $\alpha = 02^h19^m25^s0 \pm 0^s1$, $\delta = +42°07'21'' \pm 1''$, or about one beamwidth (at 8085 MHz) away from the 2695 MHz peak. Although this difference in position is barely significant, there is some basis for regarding it as a real difference. The spectral index profiles shown earlier (Fig. 11) shows that the radiation to the immediate north of the nuclear source appears to be thermal, in contrast to the nonthermal emission immediately to the south of the nuclear source. Under these circumstances, the position shift may be a direct consequence of a variation in spectral index across the nuclear region.

The 8085 MHz map shows that the nuclear region contains a small, probably unresolved (< 140 pc) source with a flux density of ~3 mJy superimposed on a complex background extending to the south, in agreement with the 2695 MHz map. Because of the low signal to noise ratio, it would be hazardous to say much more about the distribution of sources in this map.

Using a flux density of 4 mJy for the unresolved component at 2695 MHz, we obtain a luminosity of 8×10^{18} W Hz^{-1} sterad^{-1} at this frequency if $D =$ 14.3 Mpc. For comparison, we note that the luminosity of the compact nuclear sources in our own galaxy (Sag A) and M 31 are respectively 10^{17} and 2×10^{16} W Hz^{-1} sterad^{-1} at this frequency. We have assumed respective flux densities for these two sources of 150 Jy (Jones, 1974) and 3.5 mJy. The latter figure was derived from the value of 6 mJy for the nuclear source in M 31 at 1415 MHz (van der Kruit, 1972) and an assumed spectral index of 0.7. We conclude that the compact source in the nuclear region of NGC 891 is between one and two orders of magnitude more powerful than Sag A and between two and three orders of magnitude more powerful than the compact source in the nucleus of M 31.

The extended component of the nuclear source is a feature of the form also common in other spiral galaxies. Both M 31 and our own galaxy exhibit a region of relatively intense nonthermal radiation occupying a region within a few hundred parsec of the nucleus. In paper I we found that such a source exists also in Maffei 2. This source in NGC 891 appears to be a flattened region lying in the galactic plane with a brightness temperature of about 4 °K above the level of the surrounding disk when referred to the half power point (±700 pc). The mean brightness at a similar distance from Sag A is about 5 °K on the 2650 MHz map of Beard *et al.* (1969). If the surrounding disk brightness is subtracted, however, the amount attributable to the extended nuclear source in our galaxy is probably less than 1 °K. In the case of M 31 the extended nuclear source has been studied at high resolution by Pooley (1969) and van der Kruit (1972). Van der Kruit concluded that the mean brightness of this 500 pc diameter source is about 1.5 °K at 1415 MHz

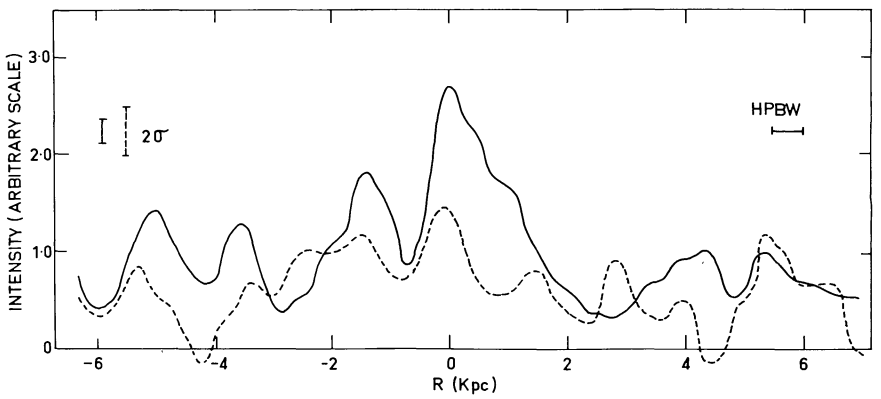

Fig. 11. Intensity profiles along the plane of NGC 891 at 2695 MHz (———) and 8085 MHz (— — —) prepared from maps with identical UV coverage. Each profile represents the brightness integrated across the galactic disk in right ascension. The error bars shown are estimates from the noise level on the maps

and is rather independent of the tilt (the source appears to be nearly spherical). At 350 pc from the nucleus his Fig. 1 shows a brightness of about 1.2 °K. If the spectral index of this region between 1415 and 2695 MHz is 0.7, as suggested by Berkuijsen and Wielebinski (1973) then the corresponding brightness temperature at 2695 MHz is 0.2 °K. We conclude that the radio emission in the nuclear region of NGC 891 is considerably brighter than the corresponding region in our own galaxy or M 31.

(e) The Galactic Disk

As we have earlier pointed out, the disk of NGC 891 appears resolved into a smooth disk component and a component made up of discrete sources. The latter component probably consists primarily of H II regions located in the spiral arms. Figure 7 shows that sources tend to "clump" together into concentrations, which supports this view. This clumping suggests that there exists a ring of emission 5 kpc from the galactic centre, and possibly another at 8 kpc. The first of these two may correspond to the ring of emission in our own Galaxy referred to as the 4 kpc arm.

The half power width of the galactic ridge, as measured in three widely separated locations free from discrete sources is about 2 ± 0.4 kpc. There is a slight broadening of the emission introduced by the inclination of the galaxy, which is 88–89° (Baldwin and Pooley, 1973), but it is insufficient to account for the large observed width. The observed thickness is comparable to the extension perpendicular to the plane of the dust filaments pointed out by Sandage (1961). The thickness of the disk observed by Baldwin and Pooley (1973) at 408 MHz is about twice the above amount if corrected to $D = 14.3$ Mpc. Therefore, there exists a component more extended at low frequencies in the Z-direction which is either resolved out or too weak to be detected in our observations. This component may possess a steeper spectrum than that of the radiation observed at 2695 MHz and would therefore be more easily observable at 408 MHz.

It is interesting that a similar effect occurs in our galaxy. For example, an inspection of the maps of Seeger *et al.* (1965) and Beard *et al.* (1969) shows that the half power angular width of the galactic emission for $l^{II} = 15°$ is about 8 degrees at 400 MHz and 4 degrees at 2650 MHz. This effect in our own galaxy is well known (cf. Pawsey, 1965) and is produced by the presence in the galactic plane of H II regions whose radiation contributes a larger fraction of the total disk radiation at 2650 than at 400 MHz. The same effect in NGC 891 supports the view presented earlier that a significant fraction of the disk radiation at 2695 MHz has a thermal origin. Baldwin (1967) has shown that the effective thickness of the plane of our galaxy at 400 MHz is 750 ± 100 pc. At 2695 MHz it would therefore be about half this width, or 375 pc. At either frequency, therefore, the width of the galactic disk in NGC 891 is about six times that in our galaxy.

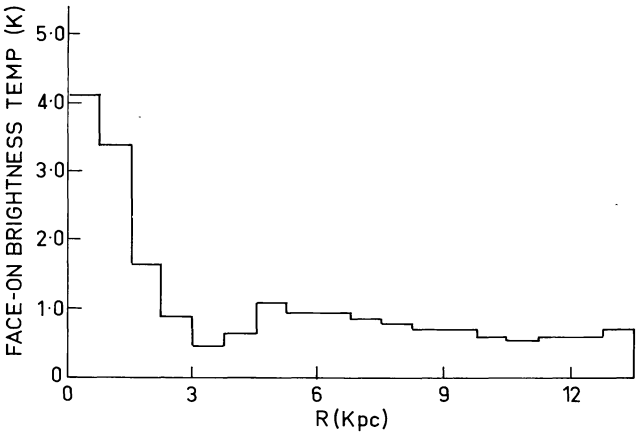

Fig. 12. Distribution of face-on brightness temperature at 2695 MHz for NGC 891 computed from the brightness integrated across the disk of the galaxy. The computations were made by averaging the profiles on opposite sides of the galactic nucleus (assumed to be coincident with the brightest point). It has been assumed that the emissivity is isotropic and distributed with circular symmetry

We may deduce the distribution of disk emissivity from the emission profile along the ridge if we assume that this distribution is circulary symmetric. If instead of the profile of the central ridge, we use the brightness integrated perpendicular to the plane of the galaxy, then it may be shown that provided the emission is isotropic, the quantity computed from this profile is equivalent to the brightness distribution as seen if the galaxy were observed face-on. If the disk thickness is independent of distance from the nucleus, it is also proportional to the volume emission coefficient. The galactic disk was divided into 18 rings, each of width 750 pc and each with its own value of emissivity which is constant for that ring. Figure 12 shows the computed distribution of face-on brightness which is required to produce the observed intensity distribution along the disk of the galaxy. A prominent feature of Fig. 12 is the pronounced dip in the brightness distribution at 4 kpc. Similar effects are observed in M 31 (Berkhuijsen and Wielebinski, 1974; Baldwin and Pooley, 1973) and NGC 4631 (Baldwin and Pooley, 1973). The brightness profile of M 51 as shown by van der Kruit (1972) also shows a similar effect. It is not clear whether this dip is produced by a local deficiency in the thermal component or the nonthermal component of the emission.

We may also compare some of the other disk features with those of other spiral galaxies. If we define a radio absolute magnitude M_R according to that given by de Jong (1967) then we obtain $M_R = -19.6$. The relation between the two magnitudes M_R and M_{pg} has been plotted for spiral, irregular and elliptical galaxies in Fig. 5 of de Jong (1967). When NGC 891 is plotted on this figure with $M_{pg} = -19.9$, we find that its radio

emission is somewhat more powerful than that expected for normal spiral galaxies.

Secondly, we may consider whether the disk emissivity is normal for spiral galaxies. Van der Kruit (1973) has compared the average face on disk brightness temperature of the "base disks" to the luminosity of the nuclear radio source, and suggests that bright disks ($T_{b\,1415} > 1\,^{\circ}\mathrm{K}$) occur exclusively in galaxies with nuclear radio sources brighter than $L_{1415} \simeq 10^{19}$ W Hz^{-1} sterad^{-1} (both parameters referred to 1415 MHz). If we assume $\beta = 0.79$ and 0.60 for the intensity spectral indices of respectively the disk and nucleus, we obtain $T_{b\,1415} = 3\,^{\circ}\mathrm{K}$ and $L_{1415} = 10^{19}$ W Hz^{-1} sterad^{-1} for NGC 891. We have probably made a slight overestimate of the disk temperature since no attempt was made to separate the base disk and spiral arm components. It is not a large overestimate however, and we conclude that NGC 891 obeys the relation suggested by van der Kruit (1973) between disk brightness and the luminosity of the nucleus.

5. Summary and Conclusions

High resolution observations of the irregular galaxy NGC 1569 and the Sb spiral NGC 891 reveal that the 2695 MHz and 8085 MHz radio emission originates in regions co-extensive with the optical forms of these galaxies. NGC 1569 is resolved into a number of emission regions many of which appear to be thermal in origin. Some of these coincide with Hα emission regions. The strongest source however contains a non-thermal component and is coincident with a continuum feature on a blue photograph of the galaxy. This source may be similar in nature to the 30 Doradus region in the Large Magellanic Cloud. There is substantial evidence that most of the radiation for NGC 1569 is thermal in origin requiring a volume emission measure of 10^{66} cm^{-3}.

The emission from NGC 891 is resolved into an extended disk and a relatively small nuclear component. Both components contain nonthermal emission. There is evidence that the nuclear region is resolved further into a flattened extended region, with diameter ~ 1400 pc, and a compact component (< 140 pc) possibly at the nucleus. The measured width (~ 2 kpc) of the galactic disk is greater than that in our own galaxy, a result which is in qualitative agreement with previous radio measurements (Pooley, 1969) and the optical appearance (Sandage, 1961). We have computed the distribution of face-on brightness temperature from the observed intensity distribution along the disk and the assumption of circular symmetry. The brightness of the disk and the power radiated by the nucleus are in agreement with the relation between these two parameters suggested by van der Kruit (1973), and adds support to the view that spirals with powerful radio nuclei possess intense disk emission.

Acknowledgements. The authors wish to express their gratitude to the NRAO staff for their generous assistance in both the observing and data reduction stages. ERS thanks the Division of Radiophysics, CSIRO, Sydney, Australia for their hospitality during the writing of the manuscript and Drs. P. W. Hodge and S. van den Bergh for providing the photographs. This work was carried out with the support of an operating grant and travel fellowship from the National Research Council of Canada (NRC) awarded to ERS, and an NRC post doctoral fellowship awarded to RCB.

References

Ables, H. D. 1971, *Publ. U.S. Naval Obs.* XX, Part IV, 60
Baldwin, J. E. 1967, IAU *Symposium No. 31*, p. 337, ed. H. van Woerden, Academic Press, London
Baldwin, J. E., Pooley, G. G. 1973, *Monthly Notices Roy. Astron. Soc.* **161**, 127
Beard, M., Thomas, B. MacA., Day, G. A. 1969, *Australian J. Phys. Astrophys. Suppl.* No. 11, p. 27
Berkhuijsen, E. M., Wielebinski, R. 1973, *Astrophys. Letters* **13**, 169
Berkhuijsen, E. M., Wielebinski, R. 1974, *Astron. & Astrophys.* **34**, 173
De Jong, M. 1967, *Astrophys. J.* **150**, 1
Gallöuet, L., Heidmann, N., Dampierre, F. 1973, *Astron. & Astrophys. Suppl.* **12**, 89
Haynes, R. F., Huchtmeier, W. K. H., Siegman, B. C., Wright, A. E. 1975, *A Compendium of Radio Measurements of Bright Galaxies*, CSIRO Division of Radiophysics Monograph, in press
Heeschen, D. S., Wade, C. M. 1964, *Astron. J.* **69**, 277
Hirabayashi, H., Yokoi, H., Morimoto, M. 1972, *Nature* **237**, 54
Hodge, P. W. 1974, *Astrophys. J. Letters* **91**, L 21
Holmberg, E. 1958, *Lund Medd* II, Nr. 136
Jones, T. W. 1974, *Astron. & Astrophys.* **30**, 37
Kazes, I., Lesqueren, A. M., Nguyen-Quang-Rieu 1970, *Astrophys. Letters* **6**, 193
Kruit, van der, P. C. 1972, *Astrophys. Letters* **11**, 173
Kruit, van der, P. C. 1973, *Astron. & Astrophys.* **29**, 249
Lequeux, J. 1971, *Astron. & Astrophys.* **15**, 30
McCutcheon, W. H. 1973, *Astron. J.* **78**, 18
McGee, R. X., Newton, L. M. 1972, *Australian J. Phys.* **25**, 619
Osterbrock, D. E., Sharpless, S. 1952, *Astrophys. J.* **115**, 140
Pawsey, J. L. 1965, Stars and Stellar Systems V, p. 219, ed. Blaauw, A., Schmidt, M., Univ. of Chicago Press, Chicago
Pooley, G. G. 1969, *Monthly Notices Roy. Astron. Soc.* **144**, 101
Roberts, M. S. 1969, *Astron. J.* **74**, 859
Sandage, A. 1961, *The Hubble Atlas of Galaxies*, Carnegie Inst. of Washington
Sandage, A., Tammann, G.-A. 1974, *Astrophys. J.* **194**, 559
Seaquist, E. R., Pfund, J., Bignell, R. C. 1975, in preparation (paper I)
Seeger, Ch. L., Westerhout, G., Conway, R. G., Hoekema, T. 1965, *Bull. Astron. Inst. Neth.* **18**, 11
Smith, M. G., Weedman, D. W., Spinrad, H. 1972, *Astrophys. Letters* **11**, 21
Vaucouleurs, G. de 1963, *Astrophys. J. Suppl.* No. 74, 31
Vaucouleurs, G. de, Vaucouleurs, A. de, Pence, W. 1974, *Astrophys. J. Letters* **194**, 119
Zwicky, F. 1971, Catalogue of Selected Compact Galaxies and of Post-Eruptive Galaxies, Speich: Zurich, p. 116

E. R. Seaquist
David Dunlap Observatory
Richmond Hill, Ontario
Canada

R. C. Bignell
Dominion Radio Astrophysical Observatory
Penticton, B.C.
Canada